World Electric Vehicle Journal

MDPI

Article

Research on the Performance of Radiators in Hybrid Vehicle Thermal Management Systems

Jiahui Li [1], Jintao Su [1,2,*] and Shuxian Wang [1]

[1] School of Automotive and Transportation Engineering, Hubei University of Arts and Science, Xiangyang 441000, China; thefies@foxmail.com (J.L.); 10835@hbuas.edu.cn (S.W.)
[2] School of Mechanical Engineering and Automation, Chongqing University, Chongqing 400030, China
* Correspondence: 11947@hbuas.edu.cn

Abstract: The cooling system plays an essential role in regulating the temperature of hybrid vehicle engines. With the contemporary surge in the number of hybrid vehicles, the cooling system's performance is vital for the safe and stable operation of these cars. The radiator, as the core component of the cooling system, has become central to enhancing thermal efficiency through performance optimization. Improvements to existing radiators are especially important in order to meet increasing performance demands. This paper firstly outlines the development of radiator technology for hybrid vehicles both domestically and internationally; it then analyzes the tube and belt radiator, and selects a louvered finned radiator with highly efficient heat dissipation performance as the object of research. It then carries out the detailed design and assessment of the radiator, formulates an accurate design scheme, and creates a three-dimensional model of the radiator and its main parts using the CATIA V5 software. Finally, the simulation and analysis Fluent software (ANSYS 2023 R1) is used to carry out a comparative analysis of the designed radiator and its important parts. The study focuses on how fin angle, inlet and outlet positioning, radiator orientation, and fan speed affect thermal performance. The findings indicate that a 26° fin angle, a same-side inlet and outlet layout, correct radiator orientation, and higher fan speeds enhance cooling efficiency. These optimizations improve radiator performance, ensuring efficient cooling under various operating conditions.

Keywords: louvered fins; thermal performance; simulation analysis

check for updates

Academic Editor: Grzegorz Sierpiński

Received: 10 January 2025
Revised: 29 January 2025
Accepted: 5 February 2025
Published: 10 February 2025

Citation: Li, J.; Su, J.; Wang, S. Research on the Performance of Radiators in Hybrid Vehicle Thermal Management Systems. *World Electr. Veh. J.* **2025**, *16*, 89. https://doi.org/10.3390/wevj16020089

Copyright: © 2025 by the authors. Published by MDPI on behalf of the World Electric Vehicle Association. Licensee MDPI, Basel, Switzerland. This article is an open access article distributed under the terms and conditions of the Creative Commons Attribution (CC BY) license (https://creativecommons.org/licenses/by/4.0/).

1. Introduction

With the rapid development of the global automotive industry and the broad adoption of vehicles, the demand for enhanced vehicle performance has become increasingly strong. Among the many factors that influence vehicle performance, the cooling system plays a crucial role in affecting the performance of hybrid electric vehicles. In the context of hybrid electric vehicles, the radiator, as a central component of the cooling system, significantly impacts the vehicle's power output, reliability, and fuel efficiency. Therefore, optimizing the design of the radiator and enhancing its heat dissipation efficiency is essential for meeting the performance requirements of modern hybrid electric vehicles.

Based on empirical methods and simplified models, traditional hybrid vehicle radiator designs often neglect complex interactions among fluid dynamics, heat transfer, and material properties. This results in suboptimal efficiency and high energy consumption, and thus the failure to meet modern hybrid automotive demands for lightweight, efficient, and environmentally adaptable systems. Consequently, utilizing scientific approaches to

optimize radiator design and enhance cooling efficiency is crucial for advancing the hybrid automotive industry.

Studies by Ashutosh et al. [1] have demonstrated that incorporating nanoscale metal oxides, particularly copper oxide, into traditional coolants can substantially improve their heat transfer capabilities. Neeti et al. [2] have shown that flat-tube radiators offer superior heat dissipation efficiency due to their increased fluid contact area, suggesting a design advantage for HEV radiators.

Building on this foundation, Arivazhagan and Balaji [3] conducted an experimental investigation into the use of a carbon-based hybrid nano-coolant in automobile radiators. Their findings indicate that this nano-fluid, composed of Graphene nanoplatelets (GnP) and multi-walled carbon nanotubes (MWCNT), enhances thermal conductivity by 59% at a 0.5% volume concentration compared to the base fluid. This enhancement leads to a notable increase in the convective heat transfer coefficient (CHTC) and an overall heat transfer coefficient (OHTC) improvement of up to 124% under optimal conditions. Despite a 23.72% increase in pressure drop, these results highlight the potential of this hybrid nano-fluid as an alternative to conventional coolants, offering significant benefits for the thermal management systems in HEVs.

Jin Huan Tai and Cui Hong Xi [4] optimized a finned multi-tube phase change material thermal energy storage system for electric vehicles in cold climates. They employed a multi-objective genetic algorithm to reduce melting/solidification times and increase energy density. Its integration into the thermal management strategy decreased energy consumption, extending vehicle range in cold conditions.

In the application of Computational Fluid Dynamics (CFD) for numerical simulation and optimized design, Liu Chao and colleagues [5] conducted research on the thermal management systems of hybrid electric vehicles, with a particular focus on the cooling issues related to nickel–metal hydride batteries. They developed a three-dimensional unsteady heat dissipation model based on the conservation laws of mass, momentum, and energy, and utilized Computational Fluid Dynamics (CFD) to perform numerical analyses of the flow and temperature fields within the battery pack.

Yu et al. (2024) [6] conducted an experimental study on this dual-cycle thermal management system for engineering radiators. Their research used Computational Fluid Dynamics (CFD) to simulate and optimize the system's design, focusing on enhancing cooling efficiency. The study supports the potential use of the dual-cycle system in improving thermal management for energy conservation and emission reduction in engineering vehicles.

Liu Haofeng and colleagues [7] utilized Computational Fluid Dynamics (CFD) to analyze the impacts of inlet and outlet positions on the performance of automotive radiators. Focusing on tube-and-fin radiators, the study assessed key structural parameters and constructed a CFD model to evaluate flow and heat transfer characteristics. The research demonstrated that fin spacing significantly affects radiator performance, and identified the optimal configuration among three different inlet/outlet arrangements to minimize fluid resistance. The findings highlight the importance of fin height and spacing for enhancing heat dissipation efficiency and the best layout for reducing coolant resistance.

In 2016, Jianzhong [8] conducted a numerical simulation of a finned radiator using the Computational Fluid Dynamics (CFD) method, and verified the accuracy of the simulation results by use of a wind tunnel test. They also optimized the design of the opening angle and spacing of the louvered fins, and found that the heat dissipation performance of the fins was significantly improved at a specific angle and spacing, which provided a new idea for the radiator design.

Research on the effects of fin thickness and height on plate-fin heat exchanger heat dissipation performance was undertaken in 2017 by Mengmeng [9]. The heat transfer factor dropped with increasing Reynolds numbers, even though increasing fin size could improve heat transfer efficiency under laminar flow circumstances. These findings serve as a guide for the numerical simulation and optimization of plate-fin radiators.

Bin [10] conducted simulation studies on the fin thickness and opening spacing of louvered fin radiators in 2018, seeking to determine the optimal parameters for flow resistance and heat transfer. In the same year, Chunhu [11] investigated the effects of louvered fin angle, direction, and arrangement on heat dissipation performance. Fluent software and wind tunnel testing were utilized to validate the simulation outcomes. He proposed an improved louvered conical structure that significantly enhanced the overall heat transfer capacity of the fins.

Maotao [12] optimized the settings of the louvered fan blades and greatly reduced their weight in a 2019 global heat transfer simulation study on passenger car louvered fin heat exchangers, based on the response surface method (RSM). By creating fins with various window angles and simulating their heat transfer and resistance properties, Guo Jianzhong and colleagues were able to increase the heat transfer effects under various window configurations effectively.

Zepeng [13] concentrated on developing a novel model of louvered fin radiators, optimizing tube-fin water-cooled radiators, and performing numerical simulations using CFD technologies in 2020. The study discovered that modifying the opening angle within a specific range might maximize heat dissipation efficiency. The orthogonal experimental design approach was used to determine the ideal combination of parameters for improving heat dissipation performance.

This study optimizes the design of louvered fin radiators for hybrid vehicles, focusing on the tube-fin type in a specific model to enhance heat dissipation efficiency. The methodology integrates literature review, numerical simulation, 3D modeling, and parameter optimization. Initially, advancements in hybrid vehicle radiator technology were reviewed to establish a theoretical basis. Subsequently, CFD simulations in Fluent and 3D modeling in CATIA are employed to analyze the radiator's fluid dynamics and heat transfer. Simulation tests adjust parameters like fin opening angle, inlet/outlet locations, placement direction, inlet water speed, and fan speed to optimize performance. The results indicate that the optimized design significantly improves heat dissipation efficiency, fulfilling modern hybrid vehicles' cooling system requirements.

2. Theoretical Foundation

2.1. Hybrid Vehicle Cooling Principle

The cooling system of a hybrid vehicle is composed of key components such as the engine, ECU, battery pack, and radiator. It manages heat through the synergistic action of coolant circulation and airflow paths to ensure the vehicle's normal operation. Temperature sensors monitor the temperature, and the control system intelligently adjusts the operation of cooling devices to maintain the optimal temperature. The system needs to be optimized to improve efficiency, intelligence, and integration, while also addressing challenges such as adaptability to high temperatures, stability under operating conditions, and cost balance. All this is shown in Figure 1.

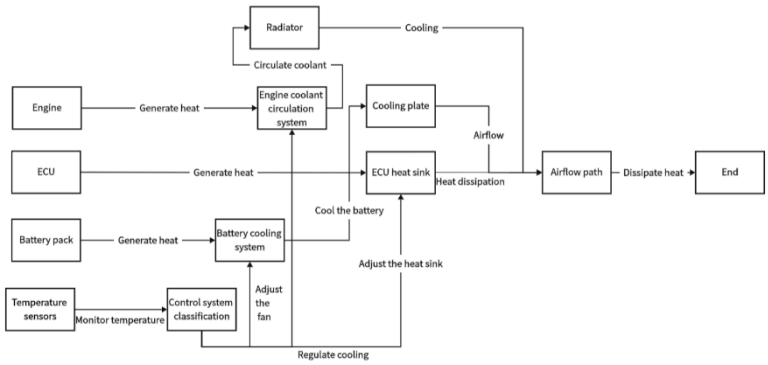


Figure 1. Hybrid vehicle cooling principal diagram.

2.2. Thermodynamic Principles of Hybrid Vehicle Radiator Operation

Conduction, convection, and radiation are the three basic mechanisms of heat transfer that make up the thermodynamic basis of radiators. Every one of these is important in making sure that the heat produced by the engine is efficiently dissipated and dispersed to the surroundings.

Heat is transmitted from one temperature field to another via the vibration, collision, or movement of free electrons within molecules, atoms, or electrons of a substance. This process is known as thermal conductivity. Conduction mostly happens through lattice vibrations, or phonons, in solids, but it also involves random molecular motion in liquids and gases. A fluid's (liquid or gas) macroscopic movement, which results in the relative displacement of its many components, is what causes convection. A natural convection cycle is produced when convection happens. Part of the fluid rises because it has expanded and become lighter due to heat, while colder, denser portions of the fluid fall. In car radiators, conduction and convection are the primary principles of heat dissipation. The coolant enters the radiator through the radiator tube walls and travels to the heat dissipation fins after exchanging heat within the engine. The heat dissipation process is then accelerated by the radiator fan's airflow across the radiator's surface.

2.2.1. Heat Exchanger Coefficient

The amount of heat transmitted per unit area of a surface per unit of time under a unit of temperature difference is described by the heat transfer coefficient, a physical number that is often represented by the Greek letter h.

The heat transfer coefficient h can be calculated using the following formula:

$$\mathrm{Q} = h \cdot \mathrm{A} \cdot \Delta \mathrm{T} \tag{1}$$

In the formula, Q represents the rate of heat transfer (unit: W); A represents the heat transfer area (unit: m^2); ΔT represents the temperature difference, which is the difference between the fluid's inlet and outlet temperatures (unit: K).

The j-factor method for the air-side heat transfer coefficient h_a [14]. is

$$h_a = j \cdot C_{p,a} \cdot G_{max} / Pr_a^{2/3} \tag{2}$$

In the formula, Pr_a is the Prandtl number for air; $C_{p,a}$ is the specific heat at a constant pair pressure; G_{max} is the maximum mass flow rate of the fluid on the heat exchanger's surface.

The j-factor for the flat tube belt-type heat exchanger is calculated using the following formula:

$$j = R_{e_{Lp}}^{-0.49} \cdot \left(\frac{\theta}{90}\right)^{0.27} \cdot \left(\frac{F_P}{L_P}\right)^{-0.14} \cdot \left(\frac{F_l}{L_P}\right)^{-0.29} \cdot \left(\frac{T_d}{L_P}\right)^{-0.23} \cdot \left(\frac{L_l}{L_P}\right)^{0.68} \cdot \left(\frac{P_t}{L_P}\right)^{-0.28} \cdot \left(\frac{\delta_f}{L_P}\right)^{-0.05} \quad (3)$$

$$Re_{Lp} = G_{\max} \cdot L_P / \mu_a \quad (4)$$

In the formula, F_P represents the fin pitch; F_l represents the fin width; θ represents the louver angle; L_P represents the louver pitch; L_l represents the louver width; T_d represents the length of the flat tube's major axis; P_t represents the tube spacing; δ_f represents the fin thickness; μ_a represents the dynamic viscosity of air.

The method for calculating the water-side heat transfer coefficient, the correlation formula for the water-side heat transfer coefficient h_1, is:

$$h_a = Nu_1 \cdot \lambda_1 / d_i \quad (5)$$

For smooth round tubes, the Nusselt number Nu_1 uses the Gnielinski correlation formula,

$$Nu_1 = \frac{(f/2)(R_{e_1} - 1000)P_{r_1}}{1 + 12.7\left(\frac{f}{2}\right)^{\frac{1}{2}}\left(P_{r_1}{}^{\frac{2}{3}} - 1\right)} \quad (6)$$

The friction factor f is calculated using the equation proposed by Petukhov,

$$f = (1.58 Ln Re_l - 3.28)^{-2} \quad (7)$$

Reynolds number is

$$Re_1 = u \cdot d_i / v_1 \quad (8)$$

In this formula, λ_1 is the thermal conductivity of water; d_i is the inner diameter of the tube; u is the velocity of water flow; P_{r1} is the Prandtl constant; v_1 is the kinematic viscosity of water.

For flat tubes, the correlation formula for the heat transfer coefficient of round tubes can also be used, but when calculating the Reynolds number, the characteristic scale d_i should be replaced with the equivalent diameter De_1 of the flat tube.

$$De_1 = 4A/U \quad (9)$$

In the formula, A represents the cross-sectional area of the flat tube; U represents the wetted perimeter.

2.2.2. Heat Transfer Coefficient

An essential metric for assessing a heat exchanger's overall heat transfer efficiency is the heat transfer coefficient, which is often represented by the letter U. The unit of measurement is usually W/(m^2·K), which indicates the amount of heat that can be transmitted via a unit area of the heat transfer surface per unit time under a unit temperature difference.

The heat transfer coefficient U can be calculated using the following formula:

$$U = \frac{Q}{A\Delta T_{lm}} \quad (10)$$

The basic heat transfer equation is

$$Q = KA\Delta t_m \quad (11)$$

In the formula, Q represents the heat transfer rate in watts (W); A represents the heat transfer area in square meters (m^2); Δt_m represents the logarithmic mean temperature difference between hot and cold fluids (°C); K is the thermal conductivity of the material, which is a material property that indicates the amount of heat per unit time that a material transfers per unit temperature difference through a unit area (usually expressed as W/(m-K)).

Exergy on the waterside can be calculated as

$$\begin{aligned} Q &= G_w C_{Pw} \Delta t_w \\ &= a_1 A_1 (t_w - t_{b1}) \end{aligned} \tag{12}$$

In the formula, G_w is the mass flow rate of water, kg/h; C_{Pw} is the specific heat of water, kJ/(kg·K); Δt_w is the average temperature difference between the inlet and outlet water and the average wall temperature, °C; a_1 is the convective heat transfer coefficient on the waterside kJ/m^2·°C; A_1 is the heat transfer area on the waterside (for a single tube), m^2; t_w is the average temperature of the water at the inlet and outlet, °C; t_{b1} is the average wall temperature on the waterside, °C.

The conduction of heat inside the pipe wall can be calculated via

$$\begin{aligned} Q &= \left(\frac{A_1'}{\frac{\tau}{\lambda_w} + \frac{\delta'}{\lambda'}} + \frac{\lambda_w}{\tau} A_m \right) (t_{b1} - t_{b2}) \\ &= \frac{1}{r} (t_{b1} - t_{b2}) \end{aligned} \tag{13}$$

In this formula, A_1' is the heat transfer area on the waterside (for a single tube), m^2; τ is the tube wall thickness, m; λ_w is the thermal conductivity of the water pipe wall, kJ/m·°C; δ' is the thickness of the solder, m; λ' is the thermal conductivity of the solder on the water pipe wall, kJ/m·°C; A_m is the area of the circular part of the water pipe wall (for a single tube), m^2; t_{b2} is the average wall temperature on the air side, °C.

The heat absorption on the air side can be calculated as

$$\begin{aligned} Q &= G_a C_{pa} \Delta t_a \\ &= a_2 \left(A_{\mathrm{I}} + A_{\mathrm{II}} \eta_f \right) (t_{b2} - t_a) \\ &= a_2 A_2 \eta_0 (t_{b2} - t_a) \end{aligned} \tag{14}$$

In the formula, C_{pa} represents the specific heat capacity of air, in units of kJ/(kg·K); G_a is the air mass flow rate, in kg/h; Δt_a is the average temperature difference between the inlet and outlet air and the wall surface, in °C; a_2 is the convective heat transfer coefficient on the air side, in kJ/m^2 °C; t_a is the average temperature of the air flow at the inlet and outlet, in °C; A_2 is the heat transfer area on the air side (for a single tube), in m^2; A_{I} is the area of the plain wall part on the air side (for a single tube), in m^2; A_{II} is the area of the fin part on the air side (for a single tube), in m^2; η_f is the fin efficiency; η_0 is the conduction of heat inside the pipe wall.

Therefore, the expression for the heat transfer coefficient U can be derived from the above formulae.

$$K = \frac{1}{\frac{A_2}{a_1 A_1} + r A_2 + \frac{A_2}{a_2 \left(A_I + \eta_f A_{\mathrm{II}} \right)}} \tag{15}$$

2.2.3. Cooling Air Volume Factor

When a vehicle is in operation, it generates cooling air in conjunction with a cooling fan, and a variety of factors need to be considered when designing a cooling system to ensure sufficient airflow to maintain the proper operation and performance of the equipment.

The actual cooling airflow can be expressed by the following equation [15]:

$$q_A = \eta q_t + q_a \tag{16}$$

In the formula, η represents the ratio of the actual air volume output by the fan to the theoretical maximum possible output; q_A is the air volume that the fan can provide under ideal conditions; q_a is the air volume generated by other factors.

Considering the heat exchange of the cooling air flowing through the radiator, if other heat dissipation formulas are not considered, the heat dissipation Q can be calculated using the following formula:

$$Q = 3600 q_w \rho_w c_{pw} \Delta t_w \tag{17}$$

The cooling air flow rate is

$$q_a = \frac{\Phi}{3600 \rho_a c_{pa} \Delta t_a} \tag{18}$$

In the formula, Δt_a is the temperature difference between the inlet and outlet of the radiator; ρ_a is the air density; c_{pa} is the specific heat capacity at the constant pressure of air.

2.3. Hybrid Vehicle Radiator Material Selection

The performance, longevity, and affordability of radiators are greatly influenced by the materials they are made of. This article examines copper and aluminum alloys, two materials frequently utilized in radiator production.

Even though aluminum alloys do not conduct heat as well as copper alloys, they nonetheless have a high enough thermal conductivity to meet most cooling requirements. Aluminum alloys have a slightly lower thermal conductivity than pure aluminum, which is around 205 W/m·K. Alloy composition and manufacturing methods have an impact on the thermal conductivity of aluminum alloys. Aluminum alloys are highly resistant to corrosion, particularly when subjected to particular surface treatments like anodizing, which can improve corrosion resistance and create a protective coating. Aluminum alloys are advantageous in terms of cost-effectiveness because their raw material and production costs are relatively low. Because aluminum alloys are lightweight, they contribute to a vehicle's total weight reduction and increase fuel efficiency.

Aluminum alloys are not as thermally conductive as copper alloys; pure copper has one of the highest thermal conductivities of any metal, at roughly 385 W/m·K. Copper alloys, which include brass and bronze, have a thermal conductivity that is considerably higher than that of aluminum alloys, but marginally lower than that of pure copper. Copper alloys are highly resistant to corrosion, particularly in saltwater and specific chemical conditions. Although copper alloys are more expensive as raw materials, their superior heat conductivity allows for the design of more efficient or compact radiators, which could lower the cost of the system. Industrial equipment, heavy-duty trucks, high-performance cars, etc., frequently use copper alloy radiators.

Consequently, the right material for a radiator should be selected depending on the radiator's heat load. Lightweight materials should be chosen for the radiator to lessen the detrimental effects on the vehicle's fuel efficiency and dynamic performance, considering the cost of the material and processing, as well as the corrosion resistance and estimated service life.

2.4. CFD Steps for Radiator Simulation Analysis

Computational Fluid Dynamics (CFD) is widely utilized in simulation studies of radiators to forecast the interior fluid flow and heat transmission mechanisms. In radiator CFD simulation studies, the following procedures are commonly used.

First, a three-dimensional geometric model of the radiator is created using geometric modeling, which guarantees that all elements, including fins, pipes, and fluid channels, are precisely represented. The next step is meshing, which forms the basis of numerical simulation. The continuous geometric model is discretized into a limited number of control volumes. The mesh's size, density, and distribution can have an impact on calculation time and simulation accuracy. In crucial regions like the fin region and the fluid inlet/outlet, finer meshes could be necessary. Boundary conditions, such as velocity inlets, pressure outlets, wall conditions (such as no-slip or partial-slip), and temperature conditions, are set after meshing.

If there is any turbulent flow in the physical model, the right turbulence model (k-ε, k-ω, or Large Eddy Simulation (LES)) needs to be chosen. The combined effects of radiation and convection may need to be considered for heat transport concerns. For the simulation results to be accurate, solver selection is essential. The flow and heat transport equations can be quantitatively solved using a solver, which is an algorithm. Different solvers, like multiphase flow solvers, PISO, and SIMPLE solvers, are usually available in CFD software (ANSYS 2023R1).

Initial conditions for the fluid domain, such as initial temperature and velocity distributions, must be set before the simulation begins. Iterative computations are carried out until the convergence conditions are satisfied, using the chosen solver and settings. Next, the temperature distribution, velocity fields, pressure drop, and heat transfer efficiency are examined in the simulation results. The results are visualized using post-processing tools like vector fields, streamline plots, and temperature contour plots.

3. Radiator Model

3.1. Types of Radiators in Hybrid Vehicles

In the cooling systems of hybrid vehicles, the radiator is a key component, primarily composed of three fundamental parts—the inlet section, the outlet section, and the heat exchange core. Radiator designs can be categorized based on the coolant flow direction into two main types—longitudinal flow and transverse flow designs. Additionally, the construction of the heat exchange core allows for further classification into various subtypes, including tube-and-fin, tube–plate, and plate–fin configurations.

The tube-and-fin radiator is characterized by an alternating arrangement of corrugated fin strips and cooling tubes, which are subsequently joined through a welding process. The fin design often incorporates small apertures reminiscent of Venetian blinds, which serve to disrupt the boundary layer formed by the airflow across the fins. Compared to tube–plate designs, tube-and-fin radiators can utilize more lightweight materials. The selection of radiator type varies according to vehicle models; for instance, passenger cars typically employ single-row tube configurations, whereas commercial vehicles often adopt double-row or multi-row tube arrangements. Such designs facilitate the adjustment of the heat dissipation area to meet the specific thermal demands of different vehicle types.

Cooling tubes and finned plates are used to produce tube–plate radiators. The tubes typically have a circular cross-section that has been flattened. These radiators are stiffer and have better structural integrity, which gives them more capacity to withstand pressure. The finned plates are usually made of thin metal sheets that are stacked in a parallel or wavy pattern. The cooling tubes are connected at their extremities to the upper and lower headers. Brazing or welding processes are used to join the plates and tubes. To maintain optimal

radiator performance, tube–plate radiators are designed with simplicity of maintenance and cleaning in mind. The inter-plate gaps facilitate convenient cleaning processes.

Plate–fin radiators enhance thermal dissipation efficiency by maximizing the heat transfer surface area, with the fins designed to possess an expansive surface area to augment contact with the ambient air. These radiators are well-suited for applications that prioritize cost-effectiveness and spatial efficiency over extreme thermal performance requirements.

Because of its unique structural arrangement, the tube-and-fin radiator is the most thermally efficient of the several design variations. This radiator is constructed by welding cooling tubes and wavy fin strips together, then carefully inspecting the weld to make sure it is strong. The tube–plate radiator, on the other hand, is made up of a set of cooling tubes with finned plates and a flattened circular cross-section. Its design maximizes the surface area available for heat dissipation while minimizing air resistance.

3.2. Determination of the Main Parameters of the Radiator

The tube-and-fin radiator can increase its heat dissipation area by around 10% in comparison to the tube–plate design, assuming the same operating circumstances. Additionally, the tube-and-fin radiator's heat dissipation fins have louvered fins that act to disrupt airflow and increase heat transfer efficiency. It is critical to produce radiators that better match the performance characteristics of contemporary automobiles, as the automotive industry is placing an increased emphasis on lightweight, all-aluminum, and integrated radiators into vehicle designs. As a result, this design was chosen because it includes louvered fins in a tube-and-fin arrangement.

This topic takes the radiator of a certain type of vehicle as the research object, and the basic parameters of the radiator for this type of vehicle are shown in the table below (Table 1).

Table 1. Structural parameters of the tube-and-fin radiator.

Parameter	Value	Unit
Core Dimensions	326 (width) × 338 (height) × 18 (thickness)	mm
Number of Cooling Pipes	25	pieces
Height of Cooling Pipes	500	mm
Number of Heat Dissipation Fins	24	strips
Length of Pipe Cross-Section	231	mm
Pipe Wall Thickness	2	mm

The structural parameters of the radiator's heat dissipation fins are shown in Table 2 below.

Table 2. Structural parameters of the heat dissipation fins.

Parameter	Value	Unit
Fins Width	20	mm
Fins Thickness	0.05	mm
Corrugation Height	12	mm
Number of Corrugations	50	pieces
Corrugation Pitch	2.6	mm
Angle of Louvered Opening θ	23	degrees

Based on the parameters, the created 3D model of the hybrid vehicle radiator is shown in Figure 2 below.

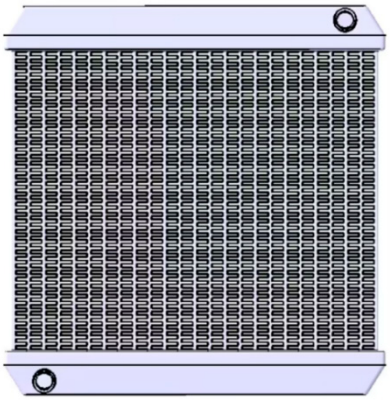


Figure 2. Hybrid vehicle radiator assembly 3D model.

The physical model of the hybrid vehicle radiator is shown in Figure 3 below.

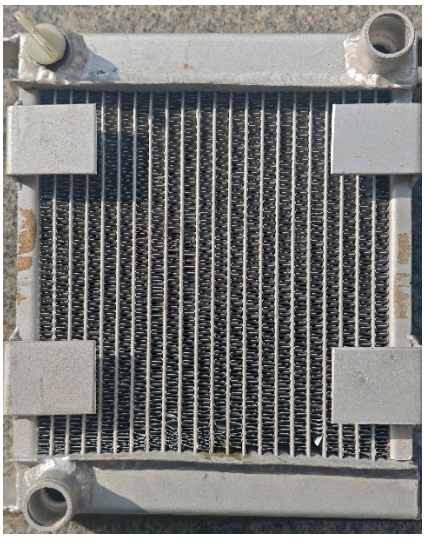


Figure 3. Physical model of the hybrid vehicle radiator assembly.

3.3. Experimental Analysis

As shown in Figure 4, in hybrid vehicles, the radiator is connected to the engine, and changes in radiator water temperature are monitored by a water temperature sensor installed at the engine water inlet.



Figure 4. Hybrid vehicle radiator arrangement and temperature sensor.

4. Experimental Method

4.1. Basic Equations for Simulation Analysis

4.1.1. Mass Conservation Equation

The law of conservation of mass is primarily applied to solve problems in thermodynamics, where heat can be transferred from one object to another, and can also be converted into mechanical energy or other forms of energy, but the total amount of energy remains constant during the conversion process. Its formula is:

$$\frac{\partial \rho}{\partial t} + \frac{\partial(\rho u)}{\partial x} + \frac{\partial(\rho v)}{\partial y} + \frac{\partial(\rho \omega)}{\partial z} = 0 \tag{19}$$

In the formula, ρ represents density; t represents time; u, v and w are the velocity components.

4.1.2. Momentum Conservation Equation

The law of conservation of momentum describes the pattern of momentum change in a fluid during motion. The commonly used conservation form of the Navier–Stokes equations is as follows:

$$\frac{\partial(\rho u)}{\partial t} + \frac{\partial(\rho u^2)}{\partial x} + \frac{\partial(\rho u v)}{\partial z} + \frac{\partial(\rho u v)}{\partial y} = -\frac{\partial P}{\partial \chi} + \frac{\partial}{\partial x}\left(\lambda \nabla \cdot \vec{v} + 2\mu \frac{\partial u}{\partial x}\right) + \frac{\partial}{\partial y}\left[\mu\left(\frac{\partial v}{\partial x} + \frac{\partial u}{\partial y}\right)\right] + \frac{\partial}{\partial z}\left[\mu\left(\frac{\partial v}{\partial z} + \frac{\partial w}{\partial x}\right)\right] + \rho f_x \tag{20}$$

$$\frac{\partial(\rho v)}{\partial t} + \frac{\partial(\rho v^2)}{\partial y} + \frac{\partial(\rho u v)}{\partial x} + \frac{\partial(\rho v w)}{\partial z} = -\frac{\partial P}{\partial y} + \frac{\partial}{\partial y}\left(\lambda \nabla \cdot \vec{v} + 2\mu \frac{\partial v}{\partial y}\right) + \frac{\partial}{\partial z}\left[\mu\left(\frac{\partial v}{\partial z} + \frac{\partial w}{\partial y}\right)\right] + \frac{\partial}{\partial z}\left[\mu\left(\frac{\partial v}{\partial z} + \frac{\partial w}{\partial y}\right)\right] + \rho f_y \tag{21}$$

$$\frac{\partial(\rho w)}{\partial t} + \frac{\partial(\rho w^2)}{\partial z} + \frac{\partial(\rho u v)}{\partial x} + \frac{\partial(\rho v w)}{\partial y} = -\frac{\partial P}{\partial z} + \frac{\partial}{\partial z}\left(\lambda \nabla \cdot \vec{v} + 2\mu \frac{\partial w}{\partial z}\right) + \frac{\partial}{\partial x}\left[\mu\left(\frac{\partial u}{\partial z} + \frac{\partial w}{\partial x}\right)\right] + \frac{\partial}{\partial y}\left[\mu\left(\frac{\partial w}{\partial y} + \frac{\partial v}{\partial z}\right)\right] + \rho f_z \tag{22}$$

4.1.3. Energy Conservation Equation

The law of conservation of energy: Assuming that external forces consist only of body forces and surface forces, the rate of change in kinetic and internal energy within a region A is equal to the work done by body and surface forces over a unit of time, plus the heat supplied to the material by the surroundings over a unit of time. In the form of the energy conservation equation for temperature, assuming the fluid is isotropic, the Fourier law of heat conduction can be derived as follows:

$$\frac{\partial \rho C_P T}{\partial t} + \nabla \cdot \left(\rho C_P T \vec{v}\right) = \nabla \cdot (k \nabla T) + s + \tau : \nabla U \tag{23}$$

In the formula, $q = -k\nabla T$; k is the thermal conductivity; C_P is the specific heat capacity at constant pressure.

4.2. Creation of the Radiator Simulation Model

4.2.1. Creating the Overall Radiator Model

The radiator under consideration is made up of 24 heat-dissipating fins and 25 heat-dissipating water pipes. In real-world situations, however, the heat-dissipation fins are louvered. The complexity of the simulation computations would increase dramatically if these fins were included in the radiator's overall simulation study. Reviewing the data reveals that, in place of the radiator tube strip, a porous medium can be used to imitate the radiator's overall heat dissipation, and the method's viability has been confirmed [16]. Consequently, the porous medium can be used for analysis instead of louvered fins. Given that replacing the fins with porous media requires determining the fins' inertial and viscous resistance coefficients, both of these must meet the requirements of the following equation:

$$\frac{\Delta^p}{\Delta z} = \frac{\mu}{\alpha} + \frac{1}{2}\rho C v^2 \tag{24}$$

In the equation, a represents the viscous resistance coefficient, C denotes the inertial resistance coefficient, and μ is the dynamic viscosity of air.

The entire radiator simulation model, as shown in Figure 5, is composed of tetrahedral meshes, with the air domain consisting of a cubic space measuring 800 mm in length, 850 mm in width, and 1282 mm in height. The radiator assembly is made up of a water chamber formed by 24 tube fins and 25 water pipes, with dimensions of 652 mm in length, 396 mm in width, and 588 mm in height. The radius of the inlet is 48 mm, and the medium within the radiator is water. The total number of mesh elements in the simulation is 5,609,165 units.

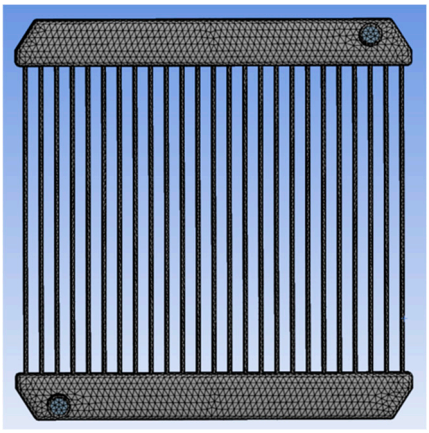


Figure 5. Overall simulation mesh model of the radiator.

4.2.2. Creating a Local Fin Model

A single fin is chosen to build a local model from the heat dissipation band, allowing the 3D modeling of this section of the heat sink belt and its louvered fins. Figure 6 and Table 3 illustrate the louvered fins' structure and specifications.

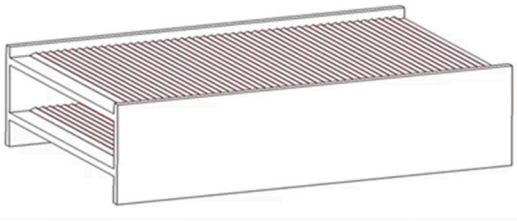


Figure 6. 3D model of the local fin.

Table 3. Model parameters of the louvered fins.

Parameter	Value	Unit
Flat Tube Width	0.4	mm
Flat Tube Length	20	mm
Fin Pitch	2.6	mm
Fin Height	12	mm
Fin Thickness	0.05	mm
Louver Angle	20~30	degrees

4.3. Simulation Analysis Presets

4.3.1. Model Settings

The analysis model employs an energy model, utilizing the relevant energy equations to establish the analytical framework. The multiphase flow model is deactivated, and the viscosity model uses the k-epsilon model, with the k-epsilon model adopting the Realizable formulation.

4.3.2. Material Settings

The fluid inside the radiator is selected to be water (liquid material), the air–fluid domain is set to air material, and the radiator model is built of aluminum material.

4.3.3. Boundary Settings

The simulation of radiator fins using the Fluent software can be difficult due to the presence of large mesh data. This can make simulation calculations extremely difficult, and may cause simulation divergence or inaccurate results. Porous media can therefore be used in place of the tube fins between the water pipes, greatly increasing the precision and effectiveness of simulation computations. Thus, a porous area with a direction defined in Cartesian coordinates replaces the heat dissipation tube fins between the radiator water pipes. The heat dissipation data for various radiator fin structures are generated by inserting the viscous resistance coefficient and inertial resistance coefficient that were derived from the simulation of the radiator's louvered fins into the formula.

For the boundary conditions of this radiator, referring to the design of the inlet for a typical passenger car radiator, the inlet temperature is set at 85 °C. Considering the outdoor temperature in Xiangyang City, Hubei Province, which is generally around 26 °C, the inlet air temperature for the radiator is designed to be 26 °C.

5. Simulation Analysis

5.1. Simulation Analysis of Different Heat Dissipation Fins

5.1.1. Local Fin Comparative Analysis

Fins with various opening angles are subjected to a comparative study. Fins at 24°, 26°, and 28° in terms of opening angle are chosen for comparison. The analysis yields the following findings in an air domain with an input velocity of 6 m/s (Figure 7): air pressure decreases as one moves deeper, because the fins, which are continually arranged and directed towards the direction of air output, are louvered. Consequently, the fin experiences the most pressure variation at its inlet position, and the smallest pressure variation at its output. It is discovered that when the opening angle increases, the pressure variation on the fins reduces when comparing fins with opening angles of 24°, 26°, and 28° under identical circumstances.

The airflow rate at various opening angles is compared based on the chosen local radiator fins under identical external conditions (as shown in Figure 8), and it is discovered that the air velocity is highest at an opening angle of 26°. Consequently, compared to other opening angles, the heat dissipation efficiency at this angle is better.

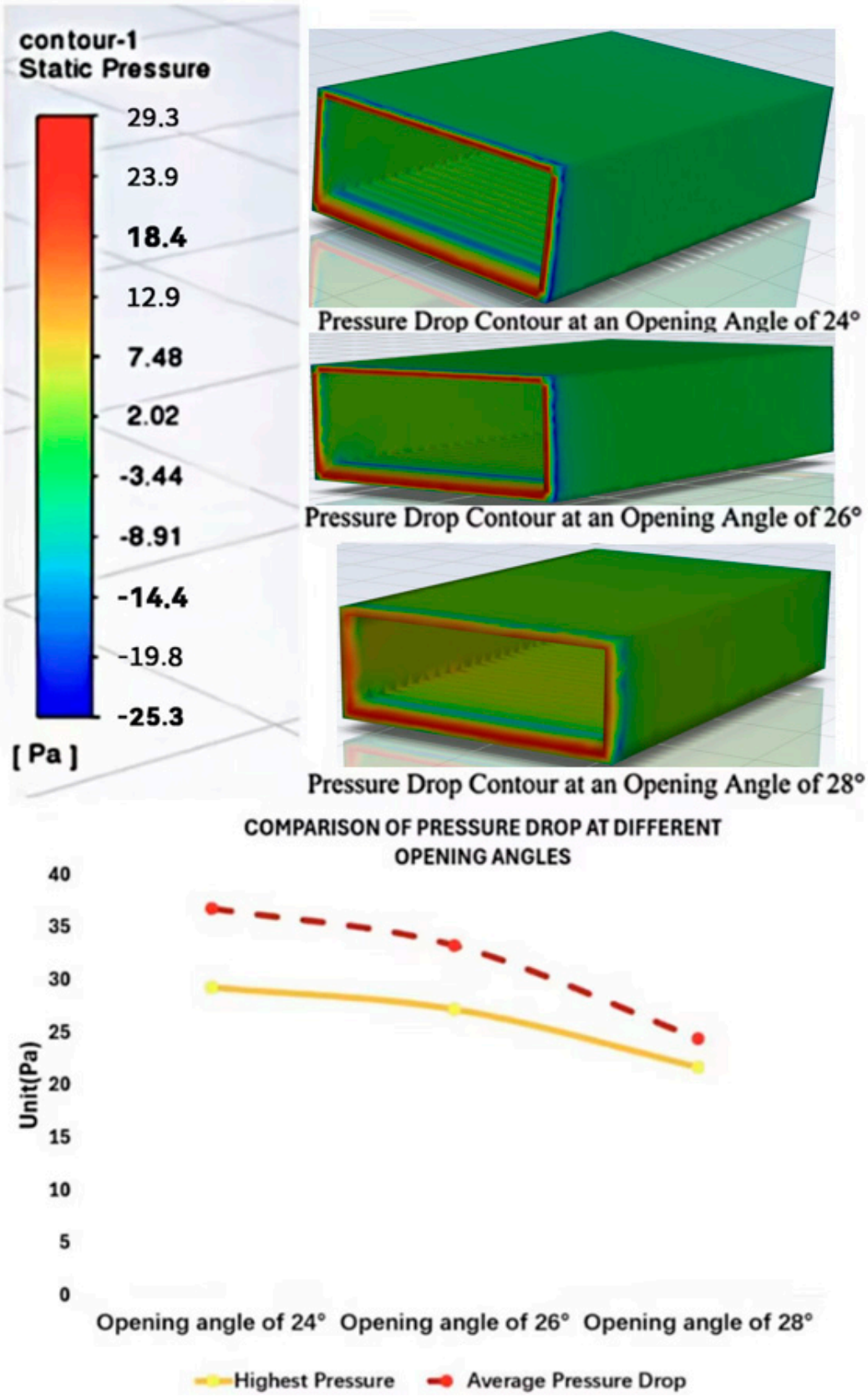


Figure 7. Analysis of the impact of opening angle on pressure drop.

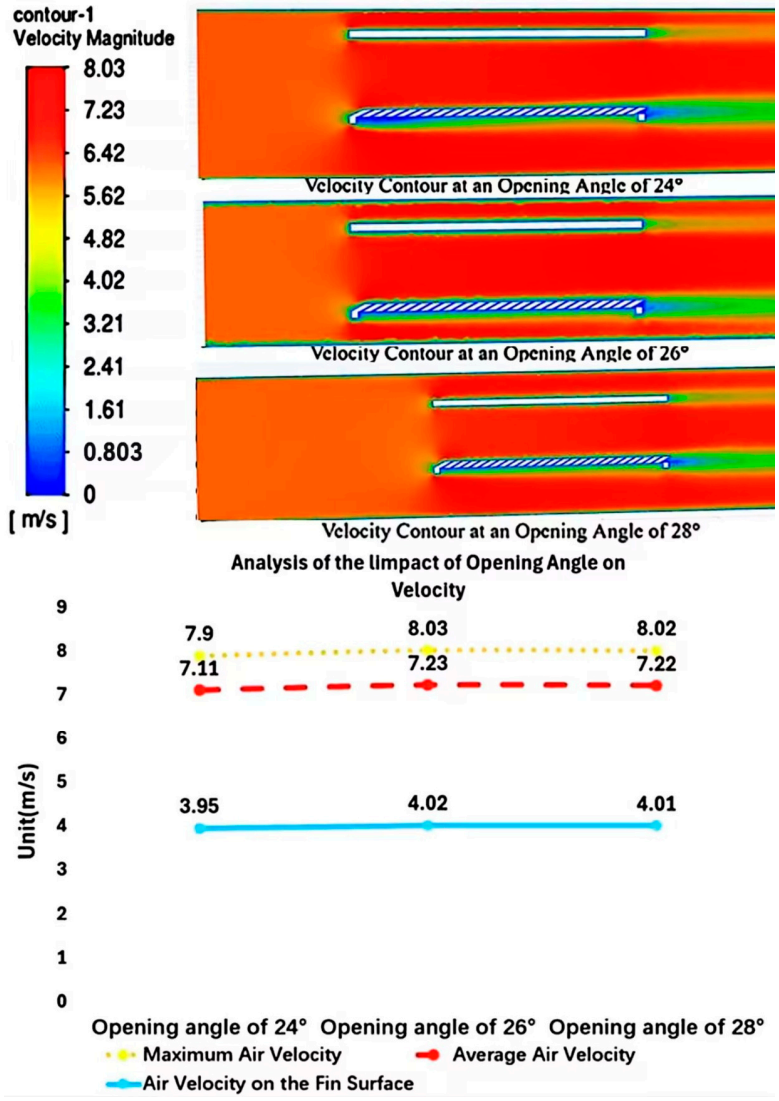


Figure 8. Analysis of the impact of opening angle on velocity.

5.1.2. Analysis of the Overall Radiator with Different Fins

The overall heat dissipation of the radiator must be calculated by introducing the resistance coefficients of the fins with various opening angles into the porous medium to compare the heat dissipation efficiency of the radiator under various fin configurations. The obtained local resistance coefficients are displayed in Table 4.

Table 4. Local resistance coefficients.

Opening Angle	Inertial Resistance Coefficient	Viscous Resistance Coefficient
24°	154.7	14,016,153
26°	180.3	14,470,745
28°	197.4	15,637,783

Incorporating the local resistance coefficients from Table 4 into the porous medium model, the simulation parameters for the radiator's air inlet were configured with a temperature of 26 °C and an incoming airflow velocity of 6 m/s. The water inlet conditions were set with a velocity of 0.6 m/s and an initial temperature of 85 °C. The simulation, employing the coupled method, was iterated 1500 times to achieve convergence.

Based on the simulation results in Figure 9, the performance distribution within the radiator was simulated using Fluent software. The results indicate that at a louver opening angle of 26° with an inlet water temperature of 85 °C, the outlet temperature drops to 71 °C, creating a temperature difference of 14 °C and an average temperature of 78.41 °C across the radiator. When the louver opening angle is adjusted to 28°, the outlet temperature increases to 72 °C, and the average temperature rises to 79.31 °C.

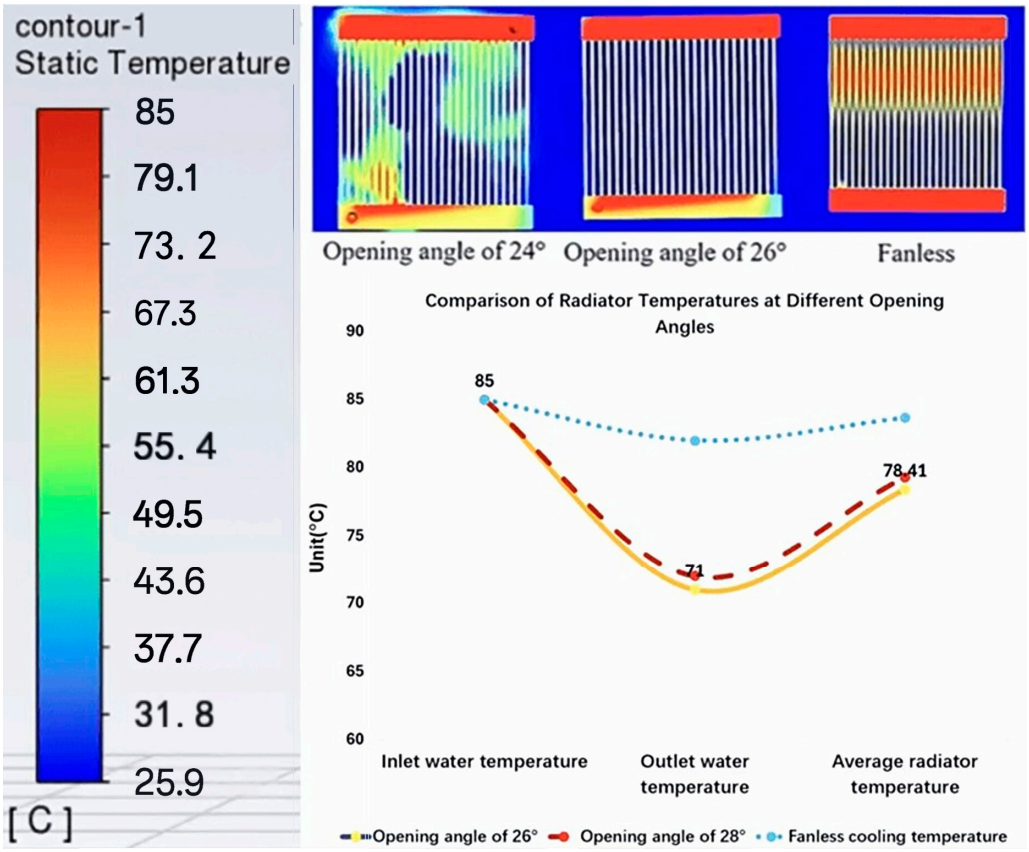


Figure 9. Radiator simulation contour map.

To isolate the fan's influence on the cooling effect, the simulation was conducted with the radiator's air inlet temperature set to 26 °C and an airflow velocity of 0 m/s. The results indicate that the outlet water temperature of the radiator increases to 82 °C, and the average temperature reaches 83.66 °C, which is significantly higher than in scenarios with fan-assisted cooling. This comparison demonstrates the crucial role of the fan in enhancing heat dissipation efficiency.

5.1.3. Simulation Analysis of Different Inlet and Outlet Positions of the Radiator

While maintaining constant environmental conditions, the impacts of varying the inlet and outlet positions of the radiator on the heat dissipation efficiency are observed. In this analysis, two radiators with different inlet and outlet positions are selected for simulation analysis (as shown in Figure 10). Different radiator arrangements are adopted for each (as shown in Figure 11), and the heat dissipation efficiency of the radiators under different arrangements is compared.

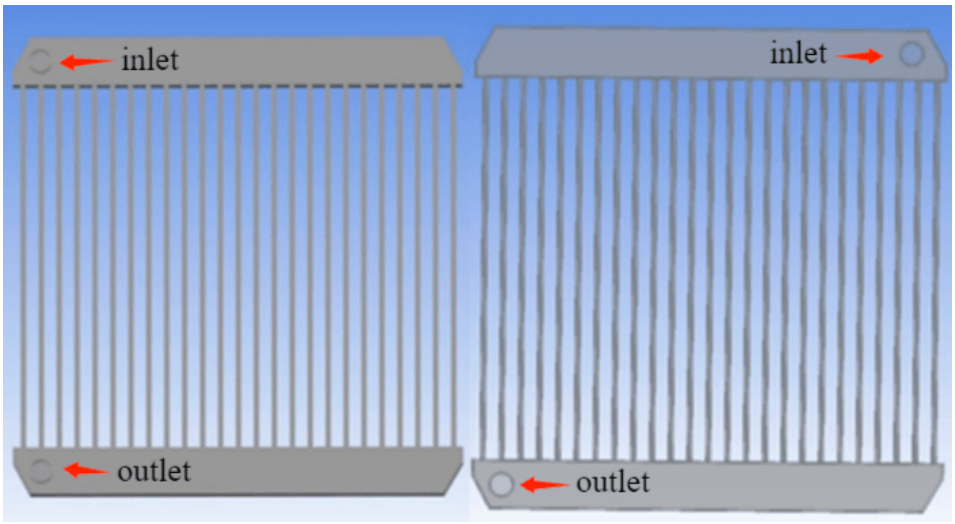


Figure 10. Radiators with different inlet and outlet positions.

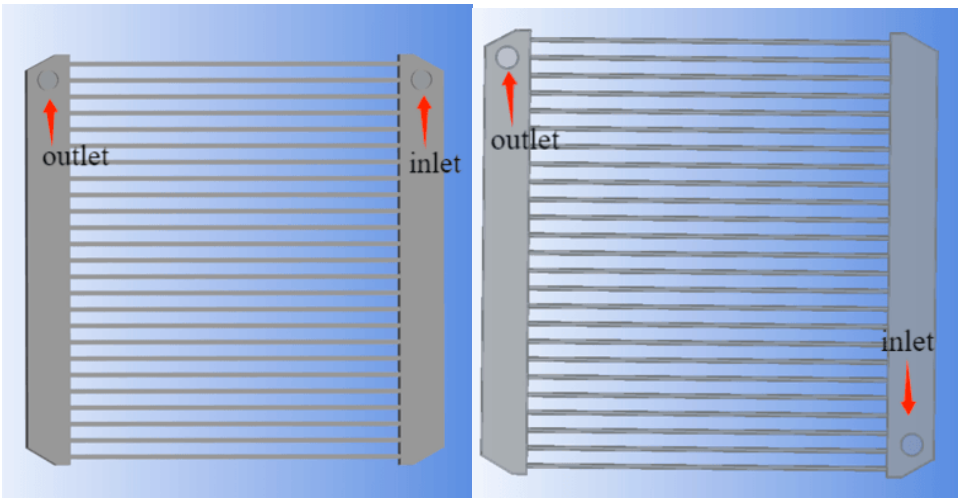


Figure 11. Radiators with different position layouts.

First, two distinct types of radiators were examined under the same environmental circumstances using Fluent for simulated analysis. The simulation technique used is in line with the previously indicated strategy, and 2000 iterations were calculated in the solution stage to see how the two distinct radiators' simulation results differed from one another.

As shown in Figure 12, with a radiator layout wherein the inlet and outlet positions were diagonal, after 2000 iterations, the inlet temperature of the radiator was 85 °C, the outlet temperature was 79.7 °C, and the average temperature of the radiator was 82.6 °C.

When a radiator configuration with the inlet and outlet locations on the same side was chosen, the radiator's average temperature after 2000 iterations was 83.6 °C, its inlet temperature was 85 °C, and its exit temperature was 81.9 °C.

In summary, by comparing different radiator layouts with varying inlet and outlet positions through simulation analysis, it was found that the radiator with a diagonally opposed inlet and outlet design exhibited slightly better heat dissipation efficiency than one with a same-side design.

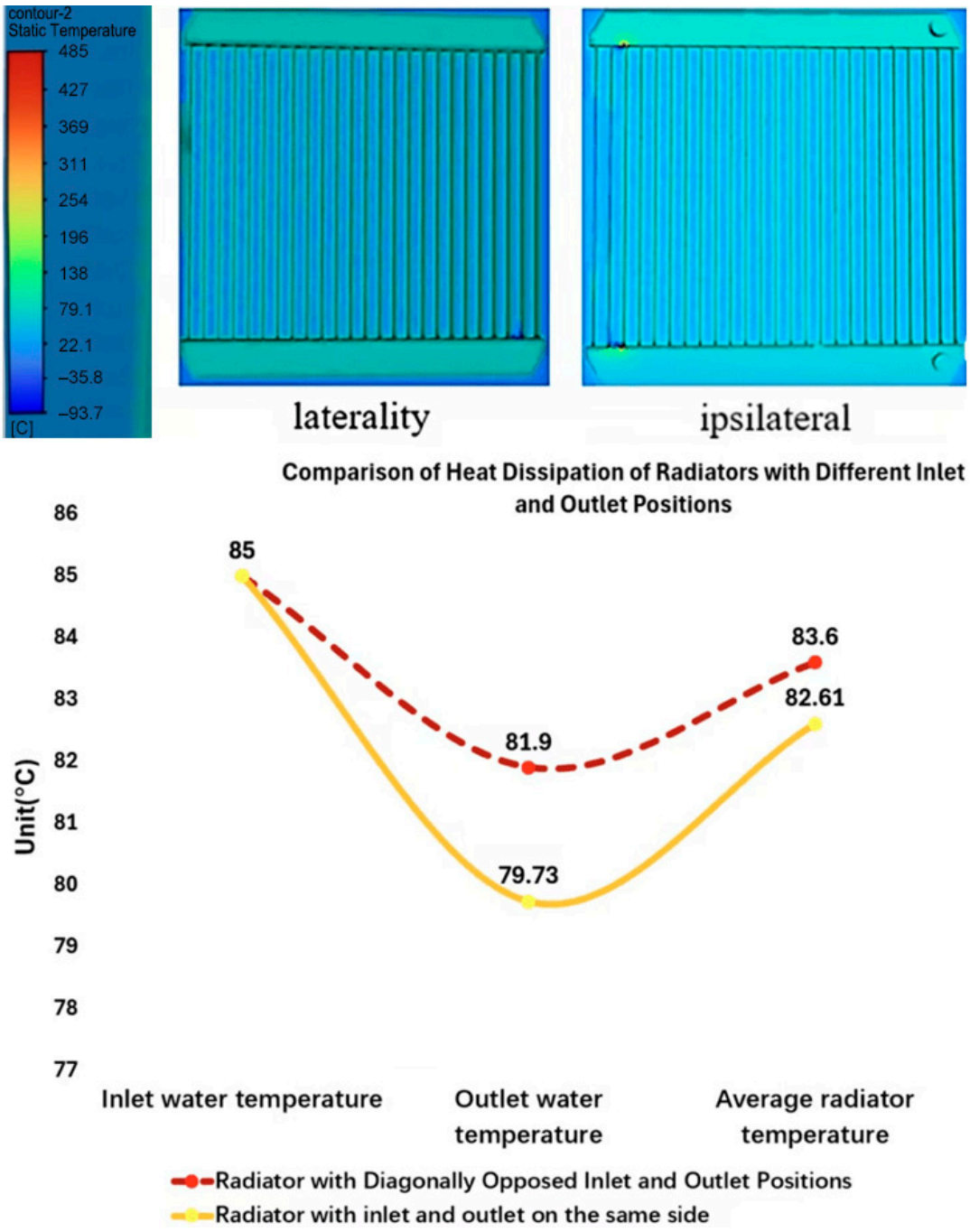


Figure 12. Simulation diagram of radiators with different inlet and outlet positions.

5.1.4. Simulation Analysis of Radiator Layouts at Different Positions

Alter the radiator had been placed in a direction that followed Figure 11's layout, we could compare the two types of radiators' effects on cooling efficiency at the same inlet velocity.

If the diagonal radiator architecture is employed, the coolant enters the bottom radiator inlet and escapes through the top radiator outlet, as seen in Figure 13. With 2000 step iterations, the internal average turbulent kinetic energy was 0.012 m^2/s^2 when the input rate was 0.6 m/s, the radiator inlet temperature was 85°, the outlet temperature was 81.7°, and the average temperature was 83.5°.

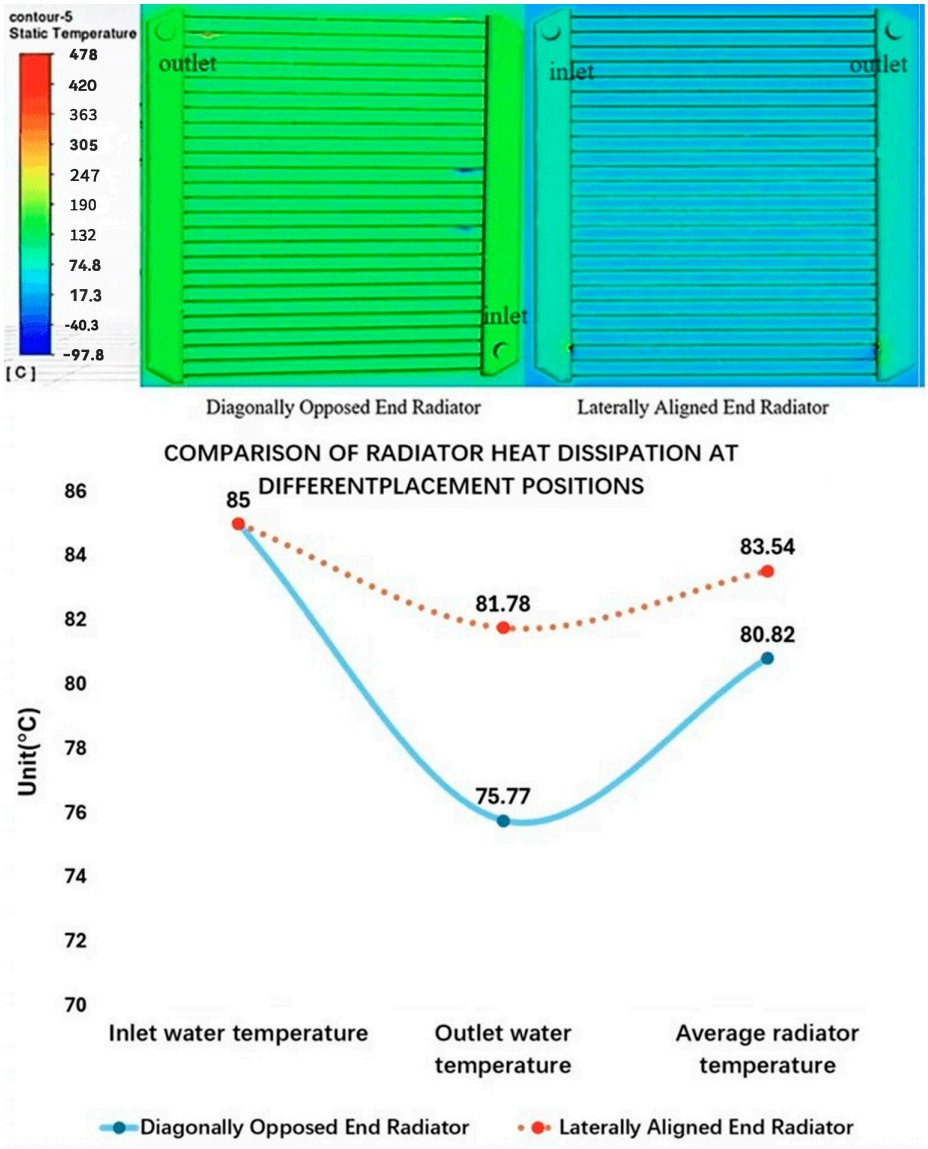


Figure 13. Simulation diagram of radiator with different position layouts.

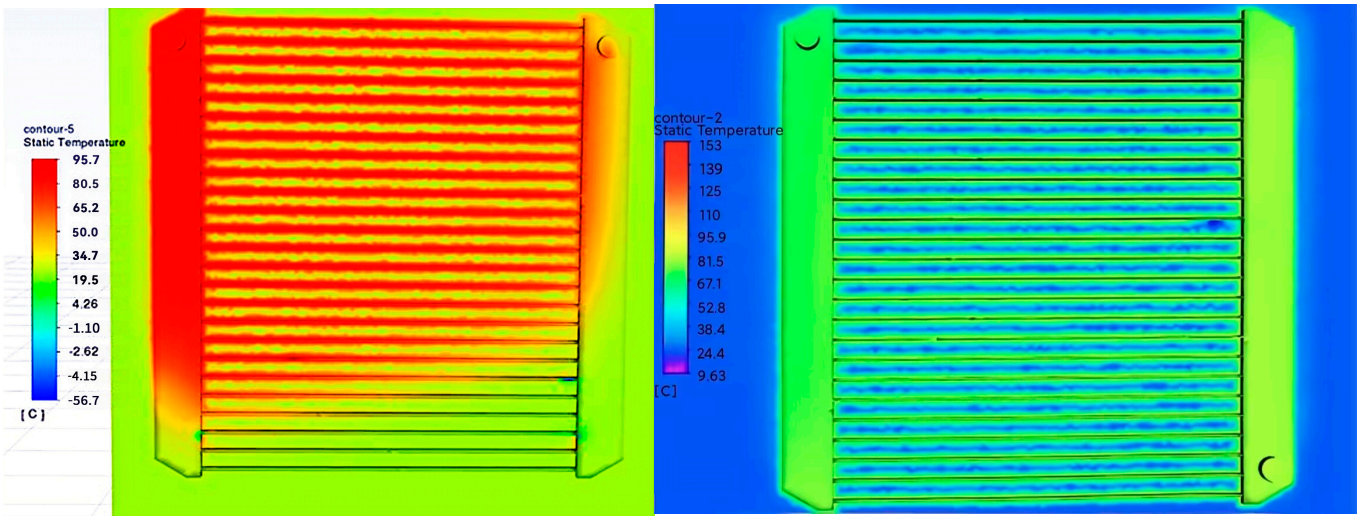
In the scenario wherein a radiator is configured with lateral inlets and outlets, the coolant flows from the right-hand inlet to the left-hand outlet. At an inlet velocity of 0.6 m/s, after 2000 iterative computational steps, the radiator exhibited an inlet temperature of 85 °C, an outlet temperature of 75.77 °C, and an average temperature of 80.8 °C, with an internal average turbulent kinetic energy quantified as 0.012 m^2/s^2.

Upon comprehensive analysis, it was observed that the radiator designed with inlets and outlets aligned on the same lateral plane demonstrated superior heat dissipation efficiency when compared to a design wherein the inlets and outlets were positioned on opposite ends. Ergo, under the specified environmental parameters, the radiator with a same-side layout configuration was more efficacious in heat dissipation.

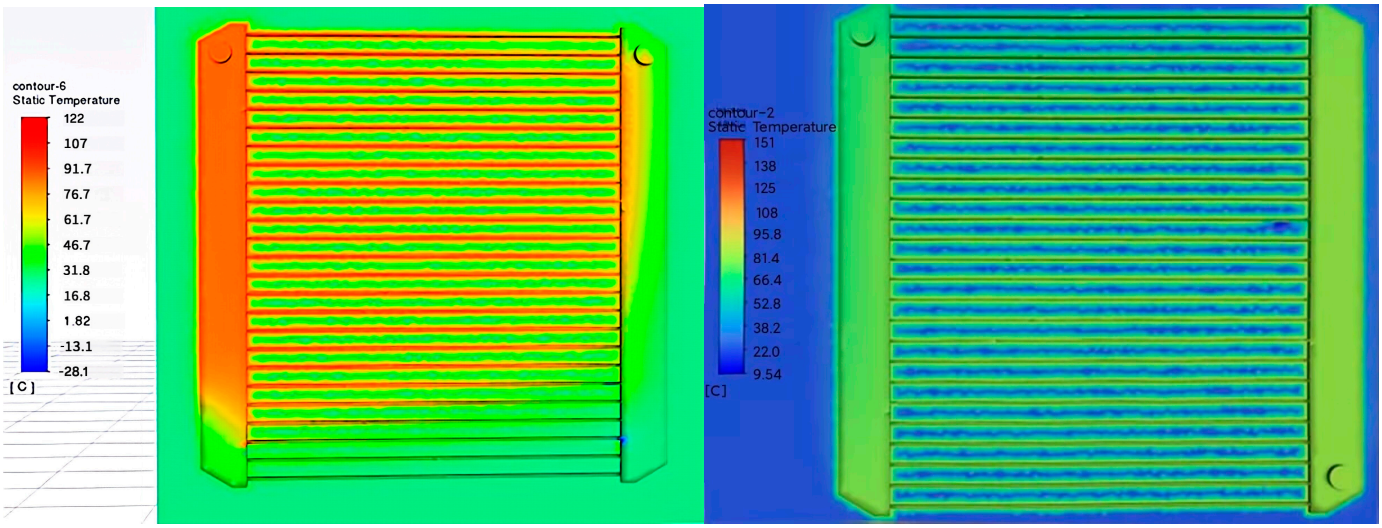
5.1.5. Simulation Analysis of Two Radiator Models Under Different Inlet Velocity Conditions

When altering the inlet velocities of the radiators to 0.8 m/s and 1.0 m/s, respectively, while keeping all other environmental conditions constant, a computational iteration of 500 steps was performed to compare the heat dissipation efficiency of the two radiator models. The radiator with inlets and outlets on the same side is hereby referred to as Radiator A, and the radiator with diagonally opposed inlets and outlets is Radiator B.

As illustrated in Figure 14, at an inlet velocity of 0.8 m/s, Radiator A exhibited an outlet temperature of 45.1 °C, an average temperature of 66.9 °C, and an internal average turbulent kinetic energy of 0.039 m^2/s^2. In contrast, Radiator B showed an outlet temperature of 71.2 °C, an average temperature of 78.7 °C, and an internal average turbulent kinetic energy of 0.018 m^2/s^2.



Simulation diagram of the radiator at an inlet velocity of 0.8 m/s.



Simulation diagram of the radiator at an inlet velocity of 1 m/s.

Figure 14. Simulation diagram of radiators with different inlet velocities.

At an inlet velocity of 1 m/s, Radiator A's outlet temperature was 52.5 °C, the average temperature was 70.27 °C, and the internal average turbulent kinetic energy was 0.026 m^2/s^2. Radiator B, on the other hand, showed an outlet temperature of 71.23 °C, an average temperature of 78.78 °C, and an internal average turbulent kinetic energy of 0.018 m^2/s^2.

The comparative analysis indicates that under the specified conditions, Radiator A, with its inlets and outlets on the same side, demonstrated higher heat dissipation efficiency than Radiator B, which had diagonally opposed inlets and outlets.

As shown in Figure 15, the heat dissipation efficiency of both radiators decreases with the increase in the inlet water flow rate. Specifically, for Radiator B, as the inlet velocity gradually increases from 0.8 m/s to 1 m/s, the outlet temperature also increases from 50.58 °C to 71.23 °C. Consequently, the heat dissipation efficiency of the radiator is related

to the inlet water flow rate. Comparative analyses between Radiator A and Radiator B reveal that Radiator A has greater heat dissipation efficiency than Radiator B, with an approximate difference of 8 °C in average temperature. Therefore, based on the Fluent results, Radiator A is shown to have a better heat dissipation efficiency.

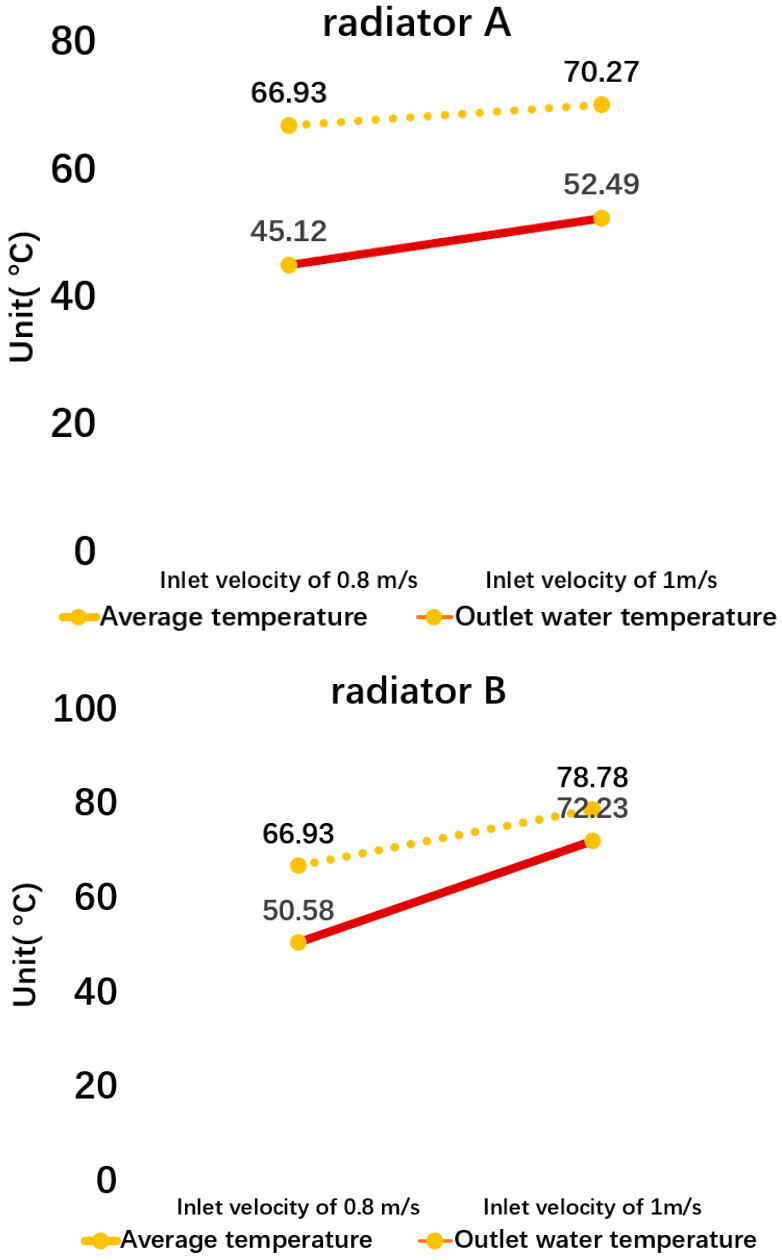


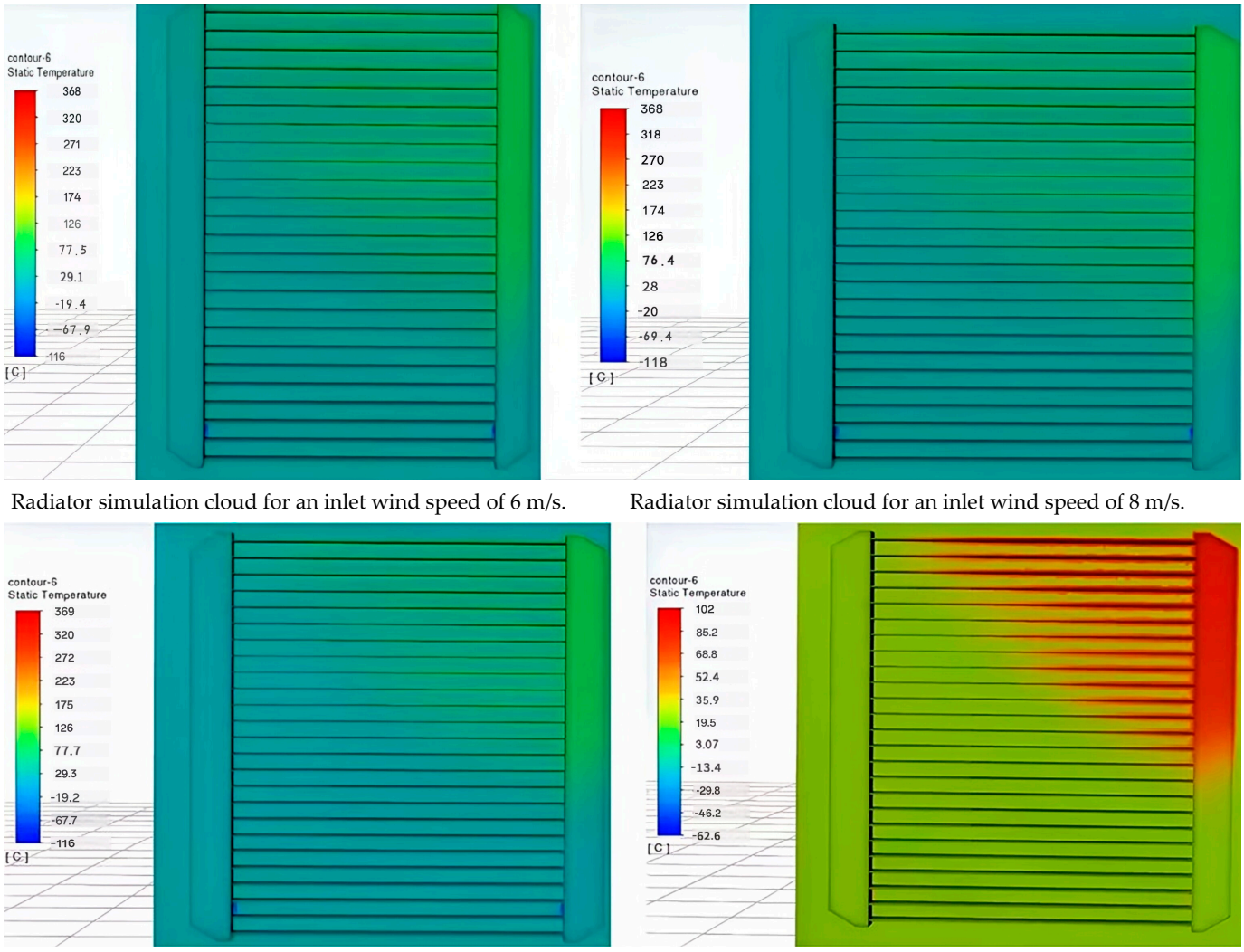
Figure 15. Fitting curves at different inlet velocities.

5.1.6. Simulation Analysis of Radiators at Different Wind Speeds

The radiator fan plays a crucial role in the heat dissipation efficiency of the radiator, and selecting the appropriate fan can enhance the radiator's cooling performance. In the following text, the same-side radiator will be taken as an example to analyze the heat dissipation efficiency of the radiator under different wind speeds.

Taking the same-side radiator from this context as an example, while keeping other environmental factors constant, the heat dissipation efficiency of the radiator is examined under wind speeds of 6 m/s, 8 m/s, 10 m/s, and 12 m/s at the inlet.

As shown in Figure 16, when the inlet wind speed was 6 m/s and the computational iteration reached 500 cycles, the outlet water temperature of the radiator was 35.3 °C, and the average temperature was 62.48 °C.



Radiator simulation cloud for an inlet wind speed of 6 m/s. Radiator simulation cloud for an inlet wind speed of 8 m/s.

Radiator simulation cloud for an inlet wind speed of 10 m/s. Radiator simulation cloud for an inlet wind speed of 12 m/s.

Figure 16. Simulation diagram of radiators at different wind speeds.

When the inlet wind speed was 8 m/s and the computational iterations reached 500 cycles, the outlet water temperature of the radiator was 30.5 °C, and the average temperature was 60.34 °C.

When the inlet wind speed was 10 m/s and the computational iterations reached 500 cycles, the outlet water temperature of the radiator was 26.9 °C, and the average temperature was 58.69 °C.

When the inlet wind speed was 12 m/s and the computational iterations reached 500 cycles, the outlet water temperature of the radiator was 26.1 °C, and the average temperature was 58.31 °C.

In summary, by analyzing the outlet temperature and average temperature of the radiator under different wind speed conditions using Fluent (as shown in Figure 17), it can be observed that the heat dissipation efficiency of the radiator increased with the increase in wind speed. The higher the wind speed, the better the heat dissipation efficiency of the radiator. Therefore, it is important to pay attention to the fan speed when the car radiator

is operating. During the high-temperature operation of the radiator, the fan speed should be increased promptly to avoid affecting the normal operation of the radiator.

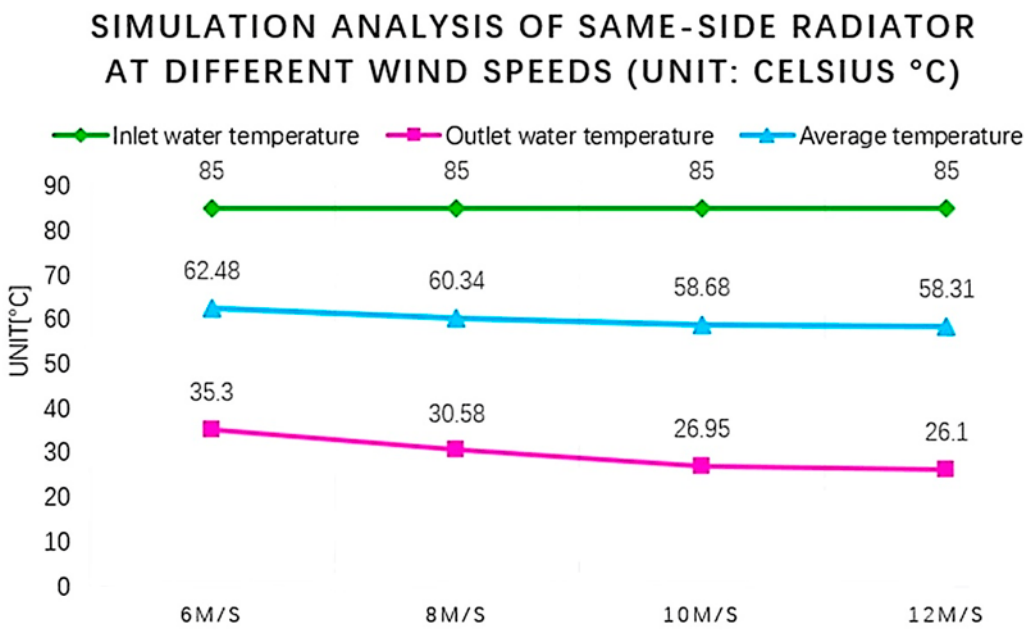


Figure 17. Temperature fitting curves at different wind speeds.

6. Simulation Results and Discussion

This paper presents a detailed simulation analysis of a hybrid vehicle radiator using Fluent software, exploring the impact of various design parameters on the radiator's performance. The following summarizes and discusses the simulation analyses results:

(1) The effect of louvered fin angles. It was determined that a fin opening angle of 26° maximizes the heat dissipation efficiency for the hybrid vehicle radiator. Increasing the angle beyond this point decreases efficiency, making a 26° opening angle the most effective choice for the fins;

(2) The impacts of radiator inlet and outlet positions. Simulations with different inlet and outlet positions revealed varying heat dissipation efficiencies. It is crucial to select an appropriate radiator layout tailored to the specific hybrid vehicle model. In this study, a same-side radiator layout was adopted, which demonstrated the highest heat dissipation efficiency;

(3) The influence of radiator orientation. Altering the orientation of the radiator showed that a configuration with coolant entering through the bottom inlet and exiting through the top outlet achieves higher heat dissipation efficiency for the hybrid vehicle radiator;

(4) The impact of fan speed on heat dissipation efficiency. The simulation results indicate that increasing the inlet wind speed significantly enhances the hybrid vehicle radiator's heat dissipation efficiency. Additionally, the radiator's performance is severely compromised when the fan is turned off, highlighting the critical role of the fan in the cooling process of hybrid vehicles.

The simulation analysis demonstrates that design parameters such as fin angles, inlet and outlet positions, orientation, inlet velocity, and fan speed all significantly affect the heat dissipation efficiency of hybrid vehicle radiators. Therefore, optimizing the design of these radiators involves setting the fin opening angle to 26°, designing the inlet and outlet positions as a same-side radiator, and orienting the radiator horizontally to align the water inlet and outlet. Adjusting the fan speed is particularly crucial under high-temperature

operating conditions, and appropriately increasing the speed can effectively enhance the cooling effect. Additionally, suction-type fans are more effective at utilizing the natural wind from hybrid vehicle movement compared to blower-type fans, thereby improving heat dissipation efficiency.

These comprehensive design optimizations aim to maximize the performance of hybrid vehicle radiators, ensuring that the vehicles maintain stable and efficient cooling under various operating conditions, thereby enhancing the overall performance and reliability of hybrid vehicles.

7. Conclusions

In this essay, an in-depth simulation analysis of the radiator of a hybrid vehicle has been carried out using Fluent software to examine the effects of various design parameters on its performance. These parameters include fin angle, position of inlet and outlet, radiator orientation and fan speed. The results show that the highest thermal efficiency was achieved with a fin opening angle of 26°. In addition, a heat sink layout with ipsilateral inlets and outlets, combined with a configuration wherein the coolant enters from the bottom and exits from the top, significantly improves cooling performance. Importantly, optimizing the fan speed proved to be a key factor in improving cooling efficiency, especially under high-temperature operating conditions.

The hybrid vehicle radiator optimized in this study offers several significant advances over the conventional radiators used in internal combustion engine vehicles. By using lightweight materials such as aluminum alloys and adopting a compact design, the radiator achieves an excellent balance between efficiency and weight. In addition, the integration of computational fluid dynamics (CFD) techniques allows for the precise optimization of heat transfer and fluid dynamics, further enhancing the adaptability of the radiator to various operating conditions.

These improvements not only meet the stringent requirements of hybrid vehicles for high efficiency, lightweight design and environmental adaptability, but also pave the way for future innovations in radiator technology. This study emphasizes the potential of exploring new materials and advanced cooling technologies (e.g., nanofluids) to push the boundaries of thermal management systems.

In conclusion, this study provides valuable insights into the design of hybrid vehicle radiators, highlighting the significant benefits of optimized design in improving cooling efficiency and overall vehicle performance. These findings highlight the potential for continued innovations in this critical area of automotive engineering.

Author Contributions: Conceptualization, J.L. and S.W.; methodology, J.L.; software, J.L.; validation, J.L. and S.W.; formal analysis, J.L.; investigation, S.W.; resources, J.S.; data curation, J.L.; writing—original draft preparation, J.L.; writing—review and editing, S.W.; visualization, J.L.; supervision, J.S.; project administration, J.S.; funding acquisition, J.S. All authors have read and agreed to the published version of the manuscript.

Funding: This research received no external funding.

Data Availability Statement: The original contributions presented in the study are included in the article, further inquiries can be directed to the corresponding author.

Conflicts of Interest: The authors declare no conflict of interest.

References

1. Kumar, A.; Hassan, M.; Chand, P. Heat transport in nanofluid coolant car radiator with louvered fins. *Powder Technol.* **2020**, *376*, 631–642. [CrossRef]
2. Arivazhagan, S.; Balaji, T. Experimental investigation of an automobile radiator using carbon based hybrid nano coolant. *Int. J. Therm. Sci.* **2023**, *193*, 108497.
3. Arora, N.; Gupta, M. An updated review on application of nanofluids in flat tubes radiators for improving cooling performance. *Renew. Sustain. Energy Rev.* **2020**, *134*, 110242. [CrossRef]
4. Kim, H.; Oh, J.; Hong, J.; Choi, H.; Kim, H.; Lee, H. Design optimization of finned multi-tube PCM heat exchanger for enhancing EV energy performance. *Appl. Therm. Eng.* **2024**, *257*, 124477. [CrossRef]
5. Liu, C.; Jia, X.; Hu, C. Design of heat sink for electric vehicle SiC MOSFET air-cooled inverter. *J. Power Supply* **2018**, *16*, 151–157. [CrossRef]
6. Yu, C.; Zhang, W.; Wang, G.; Huang, M.; Sui, J.; Zhao, H. Experimental study of dual-cycle thermal management system for engineering radiator. *Sci. Rep.* **2024**, *14*, 19691. [CrossRef] [PubMed]
7. Liu, H.; Zhao, Y.; Cao, F.; Zhao, Y. Analysis of the Impact of Inlet and Outlet Positions of Automotive Radiators Based on CFD. *Mech. Des. Manuf.* **2023**, *4*, 257–260. [CrossRef]
8. Guo, J.; Xu, M.; Zhang, G.; Hu, L.; Zhu, M.; Huang, W. Performance Analysis and Fin Structure Optimization of Automotive Radiators. *Sci. Technol. Eng.* **2016**, *16*, 58–64.
9. Pan, M. Numerical Simulation and Optimization of Plate-Fin Heat Exchanger. Master's Thesis, North China University of Water Resources and Hydropower, Zhengzhou, China, March 2017.
10. Zhang, B.; Huang, F. Influence and optimization of louvered fin structure on heat transfer characteristics of intercooler. *Guizhou Sci.* **2018**, *36*, 94–99.
11. Tian, C. Performance Simulation and Fin Optimization Design of Louvered Fin Heat Exchanger. Master's Thesis, Jiangsu University, Zhenjiang, China, 2018.
12. Zhu, M.; Tang, J.; Li, N.; Tian, C. Vehicle Cooling Fan Noise Reduction Study Using Orthogonal Test and RSM. *J. Chongqing Univ. Technol. (Nat. Sci.)* **2022**, *36*, 9–18.
13. Wang, Z.; Zhao, Z.; Miao, Z.; Ma, L.; Qiu, F. Research on heat transfer performance of water-cooled radiators with tubes and belts. *J. Refrig.* **2020**, *41*, 115–122.
14. Zhang, Z. Analysis and Simulation of the Characteristics of Tube-Core Automotive Radiators. Master's Thesis, Inner Mongolia University of Technology, Hohhot, China, 2007.
15. Lan, W.; Li, S. Thermal Field Matching Analysis of Automotive Radiator Based on FLUENT. *Mech. Des. Manuf.* **2020**, *1*, 192–195+200. [CrossRef]
16. Chang, H.; Yuan, Z. Simulation Study of Automotive Radiator Based on CFD Method. *Silicon Val.* **2009**, *19*, 8–10.

Disclaimer/Publisher's Note: The statements, opinions and data contained in all publications are solely those of the individual author(s) and contributor(s) and not of MDPI and/or the editor(s). MDPI and/or the editor(s) disclaim responsibility for any injury to people or property resulting from any ideas, methods, instructions or products referred to in the content.